ACS Macro Letters

Letter

pubs.acs.org/macroletters

Rapid, Puncture-Initiated Healing via Oxygen-Mediated Polymerization

Scott R. Zavada,[†] Nicholas R. McHardy,[‡] Keith L. Gordon,[∥] and Timothy F. Scott*[,†,§]

[†]Macromolecular Science and Engineering Program, [‡]Department of Materials Science and Engineering, and [§]Department of Chemical Engineering, University of Michigan, Ann Arbor, Michigan 48109, United States

[∥]Advanced Materials and Processing Branch, NASA Langley Research Center, Hampton, Virginia 23681, United States

Supporting Information

ABSTRACT: Autonomously healing materials that utilize thiol−ene polymerization initiated by an environmentally borne reaction stimulus are demonstrated by puncturing trilayered panels, fabricated by sandwiching thiol−ene−trialkylborane resin formulations between solid polymer panels, with high velocity projectiles; as the reactive liquid layer flows into the entrance hole, contact with atmospheric oxygen initiates polymerization, converting the liquid into a solid plug. Using infrared spectroscopy, we find that formulated resins polymerize rapidly, forming a solid polymer within seconds of atmospheric contact. During high-velocity ballistics experiments, additional evidence for rapid polymerization is provided by high-speed video, demonstrating the immediate viscosity increase when the thiol−ene−trialkylborane resins contact atmospheric oxygen, and thermal imaging, where surface temperature measurements reveal the thiol−ene reaction exotherm, confirming polymerization begins immediately upon oxygen exposure. While other approaches for materials self-repair have utilized similar liquid-to-solid transitions, our approach permits the development of materials capable of sealing a breach within seconds, far faster than previously described methods.

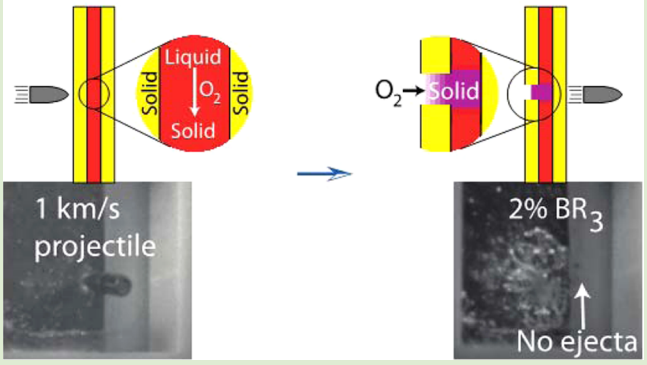

Numerous applications, spanning the biomedical, automotive, and aerospace fields, would greatly benefit from the development of polymeric materials that undergo spontaneous self-repair when damaged, extending product lifetime or preventing catastrophic failure. To date, mechanisms for the self-repair of materials have largely utilized liquid-to-solid transitions, where the action of damage to a material initiates the polymerization of an incorporated reactive liquid monomer formulation.[1−6] This reactive liquid is stored in reservoirs, such as microcapsules or capillaries, embedded in a polymeric continuous phase; the containment of the reactive liquid prevents contact with a proximate reaction stimulus, such as an initiator, catalyst, or coreactant, that could be stored either in separate reservoirs or within the continuous phase itself. Only upon application of a sufficiently high force are the walls of the capsules or capillaries disrupted, releasing the reactive liquid within and allowing it to not only flow into the damaged region but also encounter its reaction stimulus. The subsequent polymerization reaction converts the liquid into a solid which, owing to the mechanical resilience of the generated polymer, repairs and strengthens the damaged region.[1−6] While this technique has been demonstrated as a means for repairing microcracks, expanding it to other modes of healing may be advantageous, especially for materials that will automatically seal a breach formed by a high-velocity projectile. An alternative self-healing approach utilizes a solid thermoplastic polymer that, when punctured by a high-velocity projectile, partially melts to allow the passage of the projectile while retaining sufficient melt strength to permit elastic recovery; subsequent polymer chain interfusion seals the breach. For example, partially neutralized poly(ethylene-*co*-methacrylic acid) (EMAA), a relatively low modulus ionomer, undergoes puncture-induced healing at room temperature. Unfortunately, EMAA fails at temperatures greater than 60 °C, and its low modulus precludes its use in structural applications.[7,8] Conversely, poly(butadiene)-*graft*-poly(methyl acrylate-*co*-acrylonitrile) (PBG), a much stiffer material at room temperature and better suited for structural utilization, only displays puncture-healing characteristics at elevated temperatures.[9]

The puncture of a thin material, millimeters or centimeters thick, by a high-velocity projectile can be devastating under certain scenarios. For example, if the material functions as a pressurized container wall, such as in a fuel tank, an airplane hull, or the walls of a space exploration vehicle,[10] any breach causes the interior contents, whether fuel or air, to be rapidly ejected. The consequences are especially severe for manned spacecraft as the rapid loss of atmosphere would immediately endanger those inside. Systems that rely upon the mixing of

Received: May 13, 2015
Accepted: July 13, 2015
Published: July 27, 2015

DOI: 10.1021/acsmacrolett.5b00315
ACS Macro Lett. 2015, 4, 819−824

two reactive liquid components, capable of slowly filling and repairing a puncture site over several hours, have been developed;[11] however, for situations involving the breach of pressurized container walls, much faster healing mechanisms are required. Here, we describe a new autonomous-healing method to achieve extremely fast reaction rates by utilizing an environmentally borne initiation stimulus that is able to rapidly contact with and diffuse into a reactive liquid monomer formulation and effect polymerization.

Among compounds reliably present in human-occupied environments, those likely to act as initiation stimuli include water vapor (present as humidity) and other atmospheric gases (e.g., nitrogen, oxygen, carbon dioxide, etc.). Water is a well-known initiator of several polymerization reactions, most notably the anionic polymerization of alkyl cyanoacrylates utilized in commercial and medical adhesives.[12] Unfortunately, deficiencies of alkyl cyanoacrylate chemistry include its susceptibility to attack from nucleophilic species, severely limiting the choice of materials acting as liquid monomer reservoirs, as well as the sensitivity of the polymerization rate on the relative environmental humidity, where low humidity environments afford reaction rates that may prove too low[13,14] for rapid breach sealing. Of the other gases reliably present in habitable atmospheres, nitrogen and carbon dioxide exhibit very low reactivity. Conversely, oxygen is both plentiful and able to participate in radical-yielding redox reactions that are suitable for the initiation of radical-mediated polymerizations.

A notable example of oxygen's ability to rapidly yield radicals is its reaction with alkylboranes such as triethylborane and tributylborane (TBB). In the presence of oxygen, alkylboranes rapidly and exothermically produce, among other products, alkyl and alkoxy radicals (Scheme 1a),[15,16] species capable of initiating radical-mediated reactions including the chain-growth polymerization of (meth)acrylates and other vinyl monomers.[17,18] Given the extreme reactivity of alkylboranes to oxygen, even very low oxygen concentrations, such as those present as dissolved gas in monomer, are more than sufficient to initiate the reaction. This minimal requirement for oxygen is necessary as typical radical-mediated chain-growth polymerization reactions are strongly inhibited by oxygen, where the propagating radical reacts with oxygen to yield a sluggishly reacting peroxy radical.[19] Notably, Chung et al. demonstrated severe polymerization inhibition when alkylboranes were utilized in the presence of high oxygen concentrations;[17] although oxygen was required to generate the initiating species, in excess it prevented polymer growth by interfering with the propagation step, suggesting that alkylboranes are ill-suited as initiators for conventional, chain-growth radical-mediated polymerizations in environments with high oxygen concentrations.

In contrast to radical-mediated chain-growth reactions, the radical-mediated thiol−ene addition reaction between thiols and electron-rich carbon−carbon double bonds (e.g., allyl ether or vinyl ether functional groups) (Scheme 1b) is extraordinarily resistant to oxygen inhibition, a consequence of hydrogen abstraction by the peroxy radical from the ubiquitous thiol,[20] and thus is more appropriate for oxygen-mediated polymerizations.[21] Alkylboranes have previously been used to initiate coupling reactions, likely via the radical-generating alkylborane−oxygen reaction, between monofunctional thiol- and both vinyl- and alkynyl-bearing compounds;[22−25] however, initiation of thiol−ene polymerizations by alkylboranes has not been reported. Given the oxygen tolerance of the thiol−ene reaction, this polymerization mechanism is particularly amenable to the utilization of oxygen as an environmentally borne reactant with alkylboranes. To demonstrate this, the kinetics of alkylborane/oxygen-initiated thiol−ene polymerizations were examined with model thiol−ene resins, produced from difunctional thiol and allyl ether monomers (Chart 1) such that the resultant polymers were not cross-linked, using real-time FTIR spectroscopy by following the disappearance of the thiol and allyl ether absorbance peaks.[26] These model resins, mixed at 1:1 thiol:ene stoichiometric ratios, were formulated under anaerobic conditions with varying concentrations of TBB, spread as thin films on microscope slides, and placed in a gastight sample cell (Figure 1a and Figure S1, Supporting Information). As anticipated, whereas the TBB-containing formulations were stable under anaerobic conditions (Figure S2, Supporting Information), polymerizations proceeded in TBB-containing formulations immediately when air (i.e., 21% oxygen) was introduced into the sample cell (Figure 1b and Figure S3, Supporting Information); reaction rates remained rapid even at diminished oxygen concentrations (Figure S4, Supporting Information). In the absence of TBB, contact with oxygen did not induce thiol−ene polymerization, whereas increasing the TBB concentration raised both the polymerization rates and extents, an effect most evident at TBB concentrations of 1 wt % and higher. Thiol−ene polymer-

Scheme 1. Oxygen-Mediated Thiol−Ene Polymerization Mechanism and Monomer Structures[a]

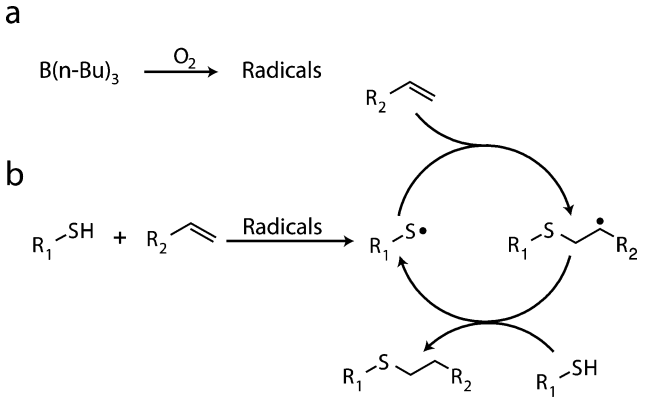

[a](a) Tributylborane reacts with oxygen to form multiple products, including alkyl and alkoxy radicals capable of initiating radical-mediated polymerizations. (b) The step-growth, radical-mediated thiol−ene reaction yields a thioether linkage from thiol and vinyl monomers through alternating propagation and chain-transfer steps.

Chart 1. Structures of Monomers Utilized in FTIR Kinetic Experiments and Ballistics Experiments

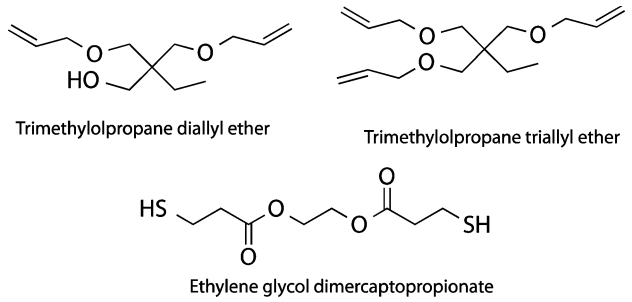

DOI: 10.1021/acsmacrolett.5b00315
ACS Macro Lett. 2015, 4, 819−824

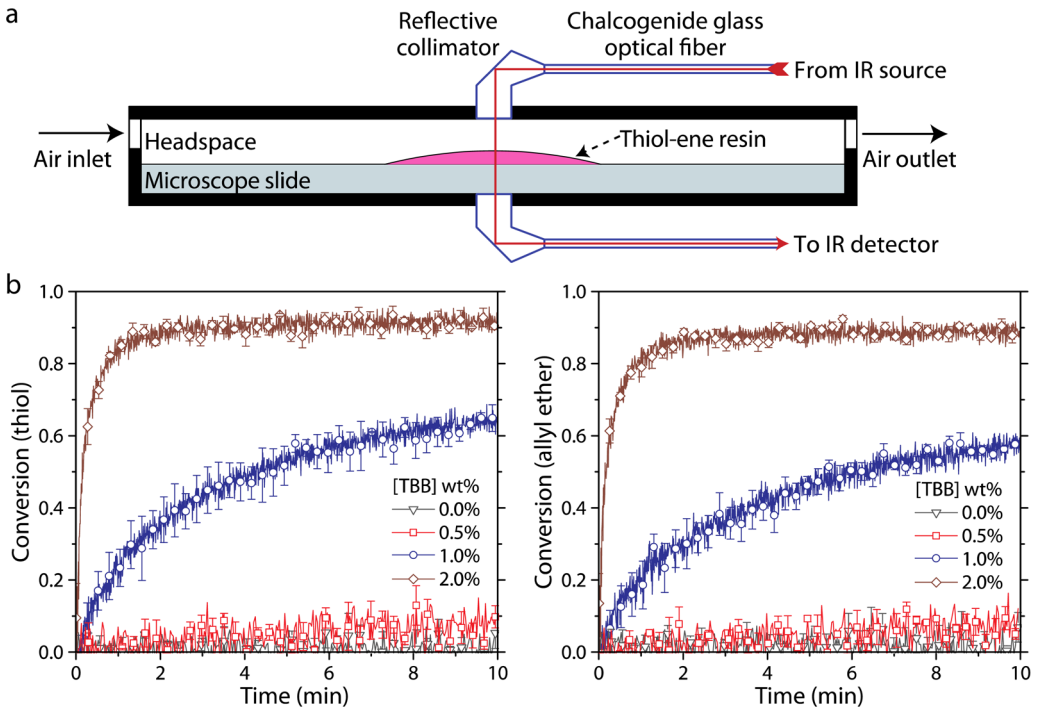

Figure 1. Reaction kinetics of oxygen-mediated thiol−ene polymerization. (a) Model thiol−ene−borane formulations, spread as thin films on glass microscope slides, were placed inside a sample cell under anaerobic conditions. Chalcogenide fiber optic cables were used to send and receive an IR beam through the sample, allowing for the reaction conversion measurement of both thiol and allyl ether functional groups. The polymerization reaction started only after air (~21% oxygen) was allowed to flow through the chamber via inlet and outlet ports. (b) Conversion versus time for thiol (left) and allyl ether (right) functional groups in EGDMP/TMPDAE resins formulated with TBB at varying concentrations upon exposure to air.

izations using multifunctional monomers formulated with TBB and contacted with oxygen lead to rapid gelation and formation of a polymer network. Notably, attempts to examine the polymerization reactions of cross-linking thiol−ene resins using IR spectroscopy were unsuccessful as the reaction itself rapidly yielded a thin, buckled skin that scattered the IR beam and resulted in poor signal-to-noise ratios; the utilization of the non-cross-linking, difunctional monomer system described above prevented the buckled surface formation. As the radical-mediated thiol−ene polymerization proceeds via step growth, the gel point can be readily predicted from the monomer functionality;[27] for example, a 3−2 monomer system (e.g., a trithiol with a diallyl ether) will gel at approximately 71% reaction conversion, a 6−2 system at approximately 45% conversion, and a 40−6 system at approximately 7% conversion. Assuming the monomer functionality does not greatly influence the pregelation polymerization rate, for the reaction conversion trajectories reported here, a thiol−ene formulation with 2 wt % TBB would gel in less than 24, 8, or 2 s by using monomer functionalities of a 3−2, 6−2, or 40−6, respectively. As evidence that the polymerization mechanism proceeds via the radical-mediated thiol−ene reaction, the thiol and allyl ether functional groups are consumed at nearly the same rate, with the thiol group consumption proceeding slightly faster than that of the vinyl groups, potentially attributable to a side reaction between thiyl radicals and butyl boranes.[16]

Having demonstrated that thiol−ene TBB formulations rapidly polymerize upon oxygen exposure, these formulations were incorporated into trilayered structures and subjected to ballistics testing to simulate micrometeoroid puncture of a spacecraft wall. The trilayered structures were constructed by sandwiching a 1 mm thick reactive liquid monomer formulation layer between two 1 mm thick solid support panels (see Figure 2a). The front, solid support panel was composed of PBG, chosen to ensure the formation of an approximately 1 mm diameter entrance hole upon projectile puncture, whereas the rear panel was composed of EMAA, a softer material that fully reseals upon ballistics puncture; this configuration permitted ready observation of the middle layer polymerization upon oxygen contact at the front entrance hole (see Figure 2a). The results of firing a projectile from a rifle at the trilayered panels were recorded with high-speed video (placed in front of and behind the sample), high-speed infrared (IR) thermal cameras to record surface temperature, or both.

The influence of varying TBB concentration (from 0 to 2 wt %), in a resin formulation utilizing EGDMP and trimethylolpropane triallyl ether (TMPTAE, Chart 1), on panel response upon puncture by a rifle-fired bullet and subsequent contact with atmospheric oxygen were initially examined using high-speed videography (Table S1, Supporting Information). A comparison of the formulations with and without TBB (Table S1, Supporting Information) revealed a striking difference in the amount of material ejected from the entrance hole (Figure 2b). For formulations omitting TBB, a plume of monomer sprayed from the entrance hole approximately 1 ms after penetration for 2.3 ± 0.8 ms. In contrast, for TBB-containing formulations, irrespective of the TBB concentration, bullet penetration yielded little to no liquid monomer ejection (see high-speed video, Supporting Information). Whereas TBB-free monomer formulations did not polymerize upon oxygen exposure, resulting in ready ejection of the low viscosity liquid resin, the rapid, radical-generating oxygen-borane reaction in TBB-containing formulations proceeds immediately upon

DOI: 10.1021/acsmacrolett.5b00315
ACS Macro Lett. 2015, 4, 819−824

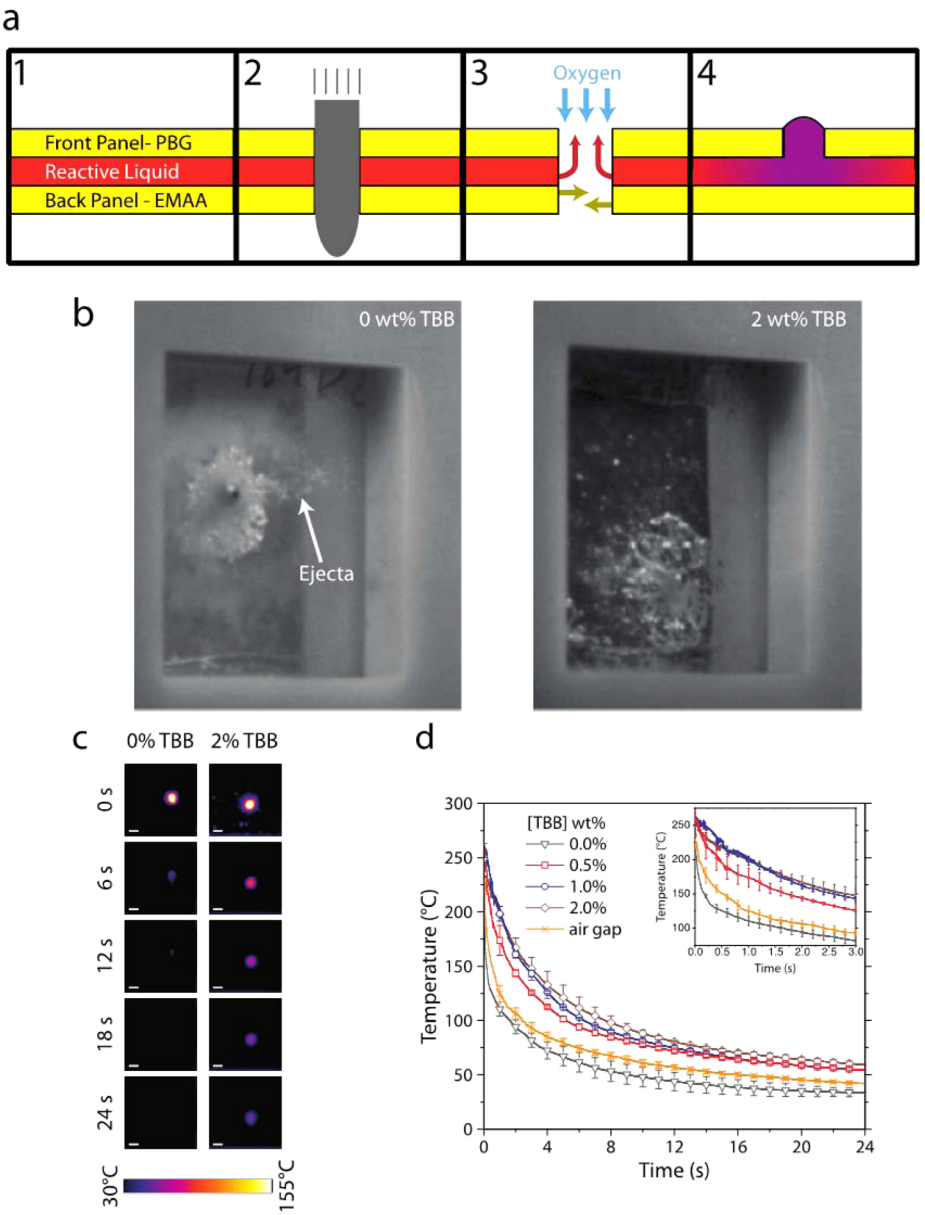

Figure 2. Ballistics testing of resin-filled panels. (a) (1) Trilayered panels, fabricated by sandwiching thiol−ene−borane resin formulations between solid polymer panels (PBG in front, EMAA at back, see text for panel and sample clamp dimensions), were (2) subjected to ballistics testing where penetration by 5.68 mm diameter bullets resulted in 1−2 mm diameter entrance holes with no exit holes; (3) as the reactive liquid layer flowed into the entrance hole, contact with atmospheric oxygen initiated polymerization, (4) converting the liquid into a solid. (b) Still images of panels and resin ejection during testing, taken from high-speed videography footage 2.5 ms after bullet impact. (c) Thermographic image series for EGDMP-TMPTAE resin-filled test panels containing 0 (left) and 2 wt % (right) TBB after bullet puncture at $t = 0$ s (scale =1 cm). (d) Maximum temperature at puncture site versus time for EGDMP-TMPTAE resin-filled test panels containing varying TBB concentrations and an unfilled test panel. Temperatures above 155 °C, outside the range of the thermal IR camera, were estimated by Gaussian fits to the temperature profiles within the camera temperature range.

oxygen exposure such that the resultant polymerization reactions and concomitant increases in viscosity[28] curtail material ejection. Postballistic inspection and videography, performed within minutes of ballistic penetration, revealed that the formulations lacking TBB remained low viscosity liquids that could be readily squeezed out the projectile entrance hole, whereas those formulated with TBB ranged from a gel (0.5 wt % TBB) to a solid, the entrance hole-filling plug (2 wt % TBB) surrounded by an approximately 1 cm diameter region of polymerized material (see video, Supporting Information, and Figure S5). Moreover, the thermomechanical properties of polymer generated from the oxygen-mediated polymerization were found to closely resemble those of a conventionally photopolymerized resin (Figure S6, Supporting Information).

Owing to the challenging experimental setup, *in situ* spectroscopic polymerization monitoring during ballistic testing proved infeasible as bullet penetration site variability risked damaging any integrated sensor necessary for measurement and potentially leading to hazardous bullet ricochet. Gordon et al. recently reported that the ballistic puncture of a PBG panel caused the surface temperature to increase by approximately 235 K,[9] attributable to projectile kinetic energy deposition into the stationary panel, and the anticipated thiol−ene polymerization employed here is exothermic.[21] Thus, panel surface

DOI: 10.1021/acsmacrolett.5b00315
ACS Macro Lett. 2015, 4, 819−824

temperatures were monitored remotely during ballistics experiments using high-speed thermography, providing a convoluted measurement of the exothermic reaction in TBB-containing resins that proceeds upon ballistic penetration and oxygen contact. Trilayered panels were constructed with reactive liquid monomer resins formulated with TMPTAE, EGDMP, and from 0 to 2 wt % TBB concentrations (Table S1, Supporting Information), as well as additional panels with the liquid resin omitted entirely, leaving a 1 mm air-filled gap. The temperature range employed to monitor the sample thermal evolution upon bullet penetration was 30−155 °C, an instrument-limited range that allowed observation of most of the temperature decay but was insufficient to capture the temperature peak immediately upon projectile impact. Consequently, the peak temperatures were established by fitting Gaussian temperature profiles across slices centered at the thermal hot spot (Figure S7, Supporting Information), such that the thermal evolution could be determined throughout the experiment, the duration of which was again instrument limited to 24 s. Using these fitted values, for the samples that contained the liquid middle layer, the maximum temperature achieved was 262 ± 6 °C, an increase of 239 ± 6 K above ambient temperature and in good agreement with the previously reported value,[9] and was not significantly influenced by the TBB concentration in samples incorporating the formulated resins. However, despite the consistency of the attained peak temperatures, direct observation of the thermal images demonstrates that the temperature decay for samples incorporating TBB-containing resins was significantly slower than the initiator-free formulation (Figure 2c and thermal IR videos, Supporting Information). This variation in temperature decay rates is highlighted in Figure 2d and Table S2 (Supporting Information), where the rate at which the penetration site temperature after bullet impact returns to ambient is markedly slower as the TBB concentration is raised. These results are readily explained by considering the oxygen-mediated, thiol−ene exothermic polymerization; upon contact with air, the TBB initiator immediately reacts with atmospheric oxygen to generate radical species that initiate the thiol−ene polymerization, releasing heat and causing the temperature to remain higher for longer when compared with TBB-free and air-gap control panels. In the absence of TBB, no polymerization reaction, and thus no exotherm, occurred upon bullet penetration, confirming that the kinetic energy deposited by the bullet in the sample was insufficient to induce polymerization and that the presence of both oxygen and TBB is necessary to initiate the reaction. Interestingly, the air-gap samples cooled more slowly than the TBB-free, resin-filled samples; this may be attributable to the lower thermal conductivity of air compared with the liquid resin, such that the air-filled samples are more thermally insulated than those filled with liquid.

The rapid reaction rates achievable by thiol−ene−alkylborane formulations, as evidenced by FTIR spectroscopy, high-speed videography, and thermography, demonstrate the potential for an environmentally borne reaction initiation stimulus to be utilized for self-healing applications. Although the model system described here was constructed from both structural (PBG) and nonstructural (EMAA and the resin itself) components, further application-oriented development of this concept would afford load-bearing walls capable of autonomous healing after multiple projectile penetration events, preserving the atmosphere inside pressurized vessels such as manned spacecraft.

EXPERIMENTAL METHODS

Real-Time FTIR Kinetics. Under oxygen-free conditions achieved in an anaerobic glovebox, rigorously degassed TMPDAE and EGDMP in a 1:1 stoichiometric functional group ratio, TBB at varying concentrations, and 0.1 wt % inhibitor (*N*-nitrosophenylhydroxylamine aluminum salt) were combined, and a 19 ± 2 μm thick layer of the formulated resin (Figure S8, Supporting Information) was deposited on a glass slide in a sealed sample cell (Figure 1c and Figure S1, Supporting Information). Infrared spectra of the formulations were monitored remotely and in transmission using a Nicolet 6700 FT-IR spectrometer equipped with a fiber optic coupling accessory via chalcogenide optical fiber patch cables (Newport Corporation catalog number 76906) fitted with silver reflective collimators (Thorlabs catalog number RC04SMA-P01); these optical fibers and collimators were employed as they permit transmission to ∼2200 cm^{-1}. The polymerization reaction proceeded only after the introduction of air (∼21% O_2) or other oxygen/nitrogen gas mixtures into the sample chamber via ports on either side (Figure S1, Supporting Information) and the reaction was monitored by observing the disappearance of the allyl ether (3100 cm^{-1}) and thiol (2570 cm^{-1}) absorbance peaks,[26] using the methyl peak at 4370 cm^{-1} as an internal standard.[29,30] Spectra were collected at a rate of two per second, whereas averaging was not required for resins formulated with 1 and 2 wt % TBB; spectra for resins formulated with 0 and 0.5 wt % TBB were averaged over four scans.

Assembly of Trilayered Sample Panels. Sample panels (75 mm × 75 mm × 3 mm) were assembled by sandwiching a 1 mm thick spacer between the edges of two 1 mm thick sheets of PBG and EMAA. The edges of the sandwich structure were then sealed using a two-component epoxy adhesive, leaving a small hole for the injection of liquid resins. In an anaerobic glovebox (<10 ppm of O_2), the reactive monomer formulations consisting of comonomers in a 1:1 thiol:ene stoichiometric ratio, TBB, and 0.1 wt % inhibitor, were mixed and injected to fill the gap between the two solid panels, after which the small injection hole was sealed using additional epoxy adhesive. The panels were stored at −20 °C during transport to the testing facility and were allowed to equilibrate for 5 min at ambient conditions prior to ballistics testing.

Ballistics. Test panels were affixed in a sample holder that clamped the panel on all edges. Bullets (0.223″ caliber full metal jacket, 3.57 g) were fired at the panels using a bolt-action rifle from 11 m away. Phantom 12 high-speed video cameras, recording at frame rates of 85 800 or 100 000 frames/s, were positioned at 45° to the entrance and exit surfaces at both the front and back of the sample. Videography analysis determined the entrance and exit bullet velocities to be 1.01 ± 0.01 and 0.97 ± 0.02 $km{\cdot}s^{-1}$, respectively. A FLIR ThermaCam SC 600 Thermal IR camera, recording over a temperature range of 30−155 °C at 500 frames per second for 24 s, was used to measure the surface temperature evolution after bullet penetration. To estimate temperatures above 155 °C, Gaussian fitting was performed on four slices of data (horizontal, vertical, and both diagonals) through the center of the thermal hot spots, and the average was reported.

ASSOCIATED CONTENT

Supporting Information

Materials and additional experimental methods. Figure S1: photographs of IR kinetics sample cell. Figure S2: reaction kinetics under anaerobic conditions. Figure S3: IR spectra of thiol−ene formulations used in kinetics experiments. Figure S4: influence of oxygen concentration on reaction kinetics. Figure S5: photographs of puncture site. Figure S6: dynamic mechanical analysis of thiol−ene polymers. Figure S7: Gaussian fitting of thermal IR data. Figure S8: measuring monomer formulation thickness. Table S1: summary of all formulations subjected to ballistics testing. Table S2: time for temperature decay after ballistics puncture. High-speed, thermal IR, and postballistics videos in .avi format. The Supporting Information

DOI: 10.1021/acsmacrolett.5b00315
ACS Macro Lett. 2015, 4, 819−824

is available free of charge on the ACS Publications website at DOI: 10.1021/acsmacrolett.5b00315.

AUTHOR INFORMATION

Corresponding Author

*E-mail: tfscott@umich.edu. Phone: (734) 763-3493.

Notes

The authors declare no competing financial interest.

ACKNOWLEDGMENTS

The authors gratefully acknowledge funding from the National Aeronautics and Space Administration (NASA Space Technology Research Fellowship, award number NNX12AM31H).

REFERENCES

(1) White, S. R.; Sottos, N. R.; Geubelle, P. H.; Moore, J. S.; Kessler, M. R.; Sriram, S. R.; Brown, E. N.; Viswanathan, S. *Nature* **2001**, *409* (6822), 794−797.
(2) Wool, R. P. *Soft Matter* **2008**, *4* (3), 400−418.
(3) Toohey, K. S.; Sottos, N. R.; Lewis, J. A.; Moore, J. S.; White, S. R. *Nat. Mater.* **2007**, *6* (8), 581−585.
(4) Dry, C. *Compos. Struct.* **1996**, *35* (3), 263−269.
(5) Pang, J. W. C.; Bond, I. P. *Compos. Sci. Technol.* **2005**, *65* (11−12), 1791−1799.
(6) Pang, J. W. C.; Bond, I. P. *Composites, Part A* **2005**, *36* (2), 183−188.
(7) Kalista, S. J. *Mech. Adv. Mater. Struc.* **2007**, *14* (5), 391−397.
(8) Varley, R. J.; van der Zwaag, S. *Acta Mater.* **2008**, *56* (19), 5737−5750.
(9) Gordon, K.; Penner, R.; Bogert, P.; Yost, W. T.; Siochi, E. *Abstr. Pap. Am. Chem. Soc.* **2011**, *242*.
(10) Brandon, E. J.; Vozoff, M.; Kolawa, E. A.; Studor, G. F.; Lyons, F.; Keller, M. W.; Beiermann, B.; White, S. R.; Sottos, N. R.; Curry, M. A.; Banks, D. L.; Brocato, R.; Zhou, L. S.; Jung, S. Y.; Jackson, T. N.; Champaigne, K. *Acta Astronaut.* **2011**, *68* (7−8), 883−903.
(11) White, S. R.; Moore, J. S.; Sottos, N. R.; Krull, B. P.; Cruz, N. A. S.; Gergely, R. C. R. *Science* **2014**, *344* (6184), 620−623.
(12) Vauthier, C.; Dubernet, C.; Fattal, E.; Pinto-Alphandary, H.; Couvreur, P. *Adv. Drug Delivery Rev.* **2003**, *55* (4), 519−548.
(13) Mankidy, P. J.; Rajagopalan, R.; Foley, H. C. *Chem. Commun.* **2006**, *10*, 1139−1141.
(14) Lewis, L. A.; Smithwick, R. W.; Devault, G. L.; Bolinger, B.; Lewis, S. A. *J. Forensic. Sci.* **2001**, *46* (2), 241−246.
(15) Liu, S. J.; Zheng, Z.; Li, M. R.; Wang, X. L. *Res. Chem. Intermed.* **2012**, *38* (8), 1893−1907.
(16) Ollivier, C.; Renaud, P. *Chem. Rev.* **2001**, *101* (11), 3415−3434.
(17) Zhang, Z. C.; Chung, T. C. M. *Macromolecules* **2006**, *39* (16), 5187−5189.
(18) Brindley, P. B.; Pearson, R. G. *J. Polym. Sci., Part B: Polym. Lett.* **1968**, *6* (12), 831−835.
(19) O'Brien, A. K.; Bowman, C. N. *Macromolecules* **2006**, *39* (7), 2501−2506.
(20) Cramer, N. B.; Scott, J. P.; Bowman, C. N. *Macromolecules* **2002**, *35* (14), 5361−5365.
(21) Hoyle, C. E.; Bowman, C. N. *Angew. Chem., Int. Ed.* **2010**, *49* (9), 1540−1573.
(22) Ichinose, Y.; Wakamatsu, K.; Nozaki, K.; Birbaum, J.-L.; Oshima, K.; Utimoto, K. *Chem. Lett.* **1987**, *8*, 1647−1650.
(23) Masuda, Y.; Hoshi, M.; Nunokawa, Y.; Arase, A. *J. Chem. Soc., Chem. Commun.* **1991**, *20*, 1444−1445.
(24) Pallela, V. R.; Mallireddigari, M. R.; Cosenza, S. C.; Akula, B.; Subbaiah, D. R. C. V.; Reddy, E. P.; Reddy, M. V. R. *Org. Biomol. Chem.* **2013**, *11* (12), 1964−1977.
(25) Sato, A.; Yorimitsu, H.; Oshima, K. *Synlett* **2009**, *1*, 28−31.
(26) Scott, T. F.; Kloxin, C. J.; Draughon, R. B.; Bowman, C. N. *Macromolecules* **2008**, *41* (9), 2987−2989.
(27) Miller, D. R.; Macosko, C. W. *Macromolecules* **1976**, *9* (2), 206−211.
(28) Chiou, B. S.; Khan, S. A. *Macromolecules* **1997**, *30* (23), 7322−7328.
(29) Westad, F.; Schmidt, A.; Kermit, M. *J. Near Infrared Spectrosc.* **2008**, *16* (3), 265−273.
(30) Hourant, P.; Baeten, V.; Morales, M. T.; Meurens, M.; Aparicio, R. *Appl. Spectrosc.* **2000**, *54* (8), 1168−1174.

DOI: 10.1021/acsmacrolett.5b00315
ACS Macro Lett. 2015, 4, 819−824